

# Combined Compression and Bending Behavior of Built-Up Columns Using High-Strength Steel



**X. Lin, K. Hayashi & M. Nakashima**

*Kyoto University, Japan*

**T. Okazaki**

*Hokkaido University, Japan*

**Y.L. Chung**

*National Kaohsiung University of Applied Sciences, Taiwan*

## SUMMARY:

The H-SA700 is a new high-strength structural steel that is more environmentally friendly and more suitable for mass production than conventional high-strength steel. A new column, built up with H-SA700 steel plates, was developed to achieve the steel construction that targets at continuous use after severe earthquake events. The column of the envisioned system is intended to serve as an elastic member, and hence should sustain large elastic deformation. This paper presents the results of a cyclic static test on the behavior of the proposed column subjected to combined bending and compression. Five specimens, varying in axial force ratio, bolt pitch near the critical section, and loading direction, were designed and examined. The column achieved an elastic rotation of 0.018 rad at the axial force ratio of 0.2, and had a maximum moment surpassing the plastic moment of the perforated section.

*Keywords: Combined compression and bending, built-up column, high-strength steel, experimental study*

## 1. INTRODUCTION

H-SA700 steel is a new structural steel that achieves very high strength without significantly altering the chemical composition (less increase in alloying elements) and without intensive heat treatment. Due to these attributes, this steel is more environmentally friendly and more suitable for mass production compared to conventional high-strength steel. The H-SA700 steel has a specified yield strength range of 700 to 900 MPa, and a specified tensile strength range of 780 to 1,000 MPa (Yoshida et al. (2009)).

A low- to mid-rise building system that allows continuous use after major earthquake events was promoted by making full use of the benefits of a new high-strength steel H-SA700. The concept drawing of the envisioned steel structural system is shown in Fig. 1. The system is achieved by connecting columns, beams and dampers using only bolts and no welds, so that all the components can be replaced, reused, and recycled. The beams can be either conventional beams using mild steel or new beams using high-strength steel. The columns are built up from H-SA700 steel plates, either flat or cold bent, using bolts exclusively and no welds. The columns are supposed to have large strength and large elastic deformation, aiming to keep elastic behavior under a very rare earthquake event.

This paper presents the experimental study on the column behavior subjected to combined constant axial force and cyclic lateral force. Five specimens were designed for three parameters, the directions of the lateral loads, the bolt pitch to fabricate the column and the magnitude of the axial force exerted on the column. The specimens were reduced in dimension from the prototype section used in the writers' previous research (Lin et al. (2011)). The effect of different parameters on column behavior, such as stiffness, elastic deformation capacity, strength and failure modes, were evaluated.

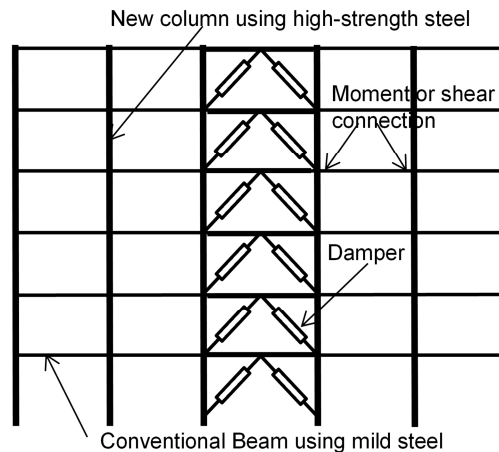


**Figure 1.** Concept of structural system.

## 2. EXPERIMENTAL PROGRAM

### 2.1 Specimens and test setup

Fig. 2 shows the baseline specimen and the test setup. The column consists of two plates and two cold-formed channels, and is built using high-strength bolts (see Fig. 2(a)). The bolts had a nominal diameter of 8 mm and a specified minimum tensile strength of 1,220 MPa. Five specimens with the same section of 110 mm × 110 mm were constructed. The parameters of the specimens are listed in Table 1. Since the column was intended for use in the elastic range, the elastic deformation capacity, elastic stiffness, and the safety margin above the elastic limit were the main concerns for specimen design. There were three parameters, lateral load direction (about the strong or weak axis, bolt pitch (60 mm or 120 mm) near the critical section, and axial force ratio (0.0, 0.2 or 0.4). The baseline specimen (denoted as X60N2) was loaded about the strong axis (X-axis), and had a bolt pitch of 60 mm and an axial force ratio of 0.2. The axial force ratio is defined as the ratio of the axial compressive force to the axial compressive yield strength of the gross cross-sectional area. Larger bolt pitch may cause an early local buckling, and hence reduce the strength of the column, while larger axial force may affect the stiffness, strength, and yield rotation. The exterior plate of the flange between two adjacent reduced sections was more critical to buckling. Lin et al. (2011) shows its buckling can be well estimated by the elastic column buckling theory, taking each bolt pitch as the column length, and assuming that the ends are fixed against rotation (due to the channels preventing the exterior plates to buckle into the section). The critical stress for the local buckling of the exterior plate was 1,684 MPa for the specimen with a bolt pitch of 60 mm, and 6,737 MPa for specimens with a bolt pitch of 120 mm, so the specimens were expected to avoid local buckling of the exterior plate before yielding. The material properties of the steel plates for the specimens are shown in Table 2. The H-SA700 steel had a rupture elongation of about 13%, which is only half of that of conventional mild steel, and a yield ratio (the ratio of the yield stress to tensile stress) of 0.94, which indicates limited strength increase beyond the yield stress.

The loading system in Fig.2(c) was adopted to provide the combined action of bending and compression to the column. The top end of the 2-MN vertical oil jack was fixed to a reaction beam, while the bottom fixed to the top end plate of the column through oil jack connector. The right side of the 200-kN horizontal jack was fixed to a reaction frame, while the left side to the oil jack connector. The specimen was placed into the setup, and connected to the base and the oil jack connector by end plates. To simplify the connection between the loading system and the column, the end plate was welded to the column. Two base components were bolted to clamp the bottom of the column to present the boundary conditions for bolted connections, e.g., bolted column base or extended end-plate beam-to-column connection (Lin et al. (2012)). Two stiffeners that were made of H-SA700 steel were welded to the internal channels to avoid the large local deformation and damage in the connection

between the column and base components.

**Table 1.** Specimens

Specimen No.	Load direction	Bolt pitch(mm)	Axial force ratio $N/N_0$	Instructions
X60N0	X	60	0.0	No axial force
X60N2	X	60	0.2	Baseline Specimen
X60N4	X	60	0.4	Larger axial force
X120N2	X	120	0.2	Larger bolt pitch
Y60N2	Y	60	0.2	Different load direction

**Table 2.** Material Properties

Specimen No.	Thickness (mm)	Yield Stress $F_y$ (MPa)	Tensile Stress $F_{max}$ (MPa)	Yield Ratio $F_y/F_{max}$	Rupture Elongation
X60N0, X60N2, X60N4, X120N2	6.0	803	851	0.94	13%
Y60N2	6.0	787	833	0.94	13%

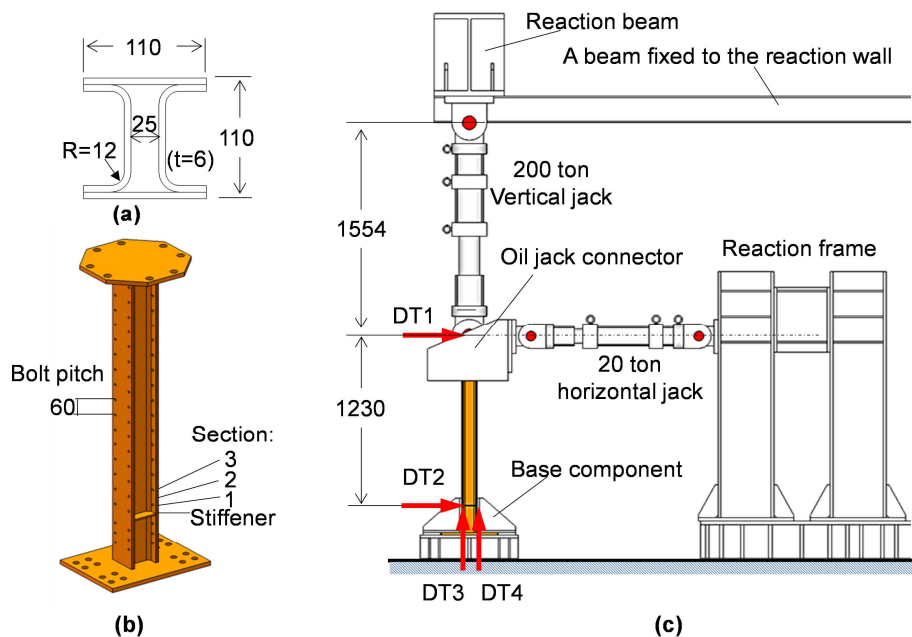


**Figure 2.** Specimens and setup (unit: mm).

## 2.2 Instrumentation and Test procedure

The segment of the column above its stiffeners was measured as the tested portion, which excluded connections at the bottom. The height of the column was taken as the distance from the stiffener to centreline of the horizontal jack (1,230 mm). Two displacement transducers, DT3 and DT4, were used to measure the deflection angle at the stiffeners, and other two, DT1 and DT2, were used to obtain the drift of the column, as shown in Fig.2(c).

Cyclic loading was applied to all the columns. The loading protocol for the lateral drift of the column was as follows: two cycles for each story drift ratio (called as SDR hereafter) of  $\pm 0.005$ ,  $\pm 0.01$ ,  $\pm 0.02$ ,  $\pm 0.03$ ,  $\pm 0.04$ ,  $\pm 0.06$ ,  $\pm 0.08$  rad and finally three cycles of  $\pm 0.10$  rad. The story drift ratio here is the ratio of the drift to the column height. The loading could also be terminated due to severe local buckling or rupture in the column.

## 3. ANALYSIS OF THE RESULTS

Fig.3 shows the moment versus rotation relationship for each specimen. The moment uses the bending moment of the column at the first perforated section from the stiffener (Section 1 in Fig. 3(b)), which was expected as the most critical section to yielding and rupture. The column rotation was obtained by subtracting the deflection angle of the bottom stiffeners from the story drift angle of the column. Three types of markers were used to indicate the instants when local buckling, plate fracture, or bolt fracture was observed. Fig.4 presents the photos for the final failure state of each specimen. The arrows in the photos indicate the locations where fracture occurred.

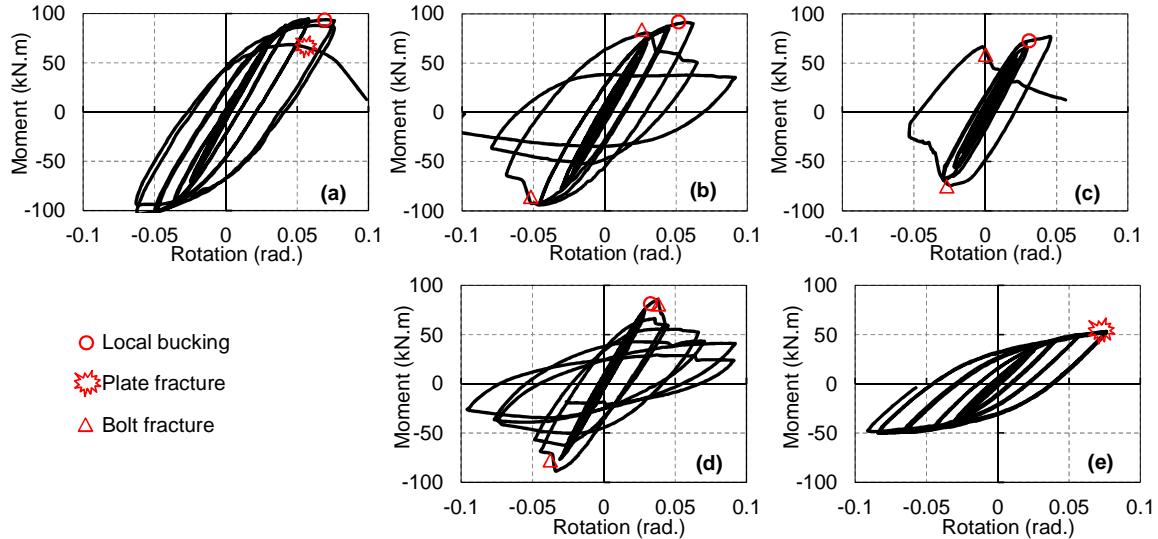


**Figure 3.** Moment versus rotation relationship: (a) X60N0; (b) X60N2; (c) X60N4; (d) X120N2; (e) Y60N2.

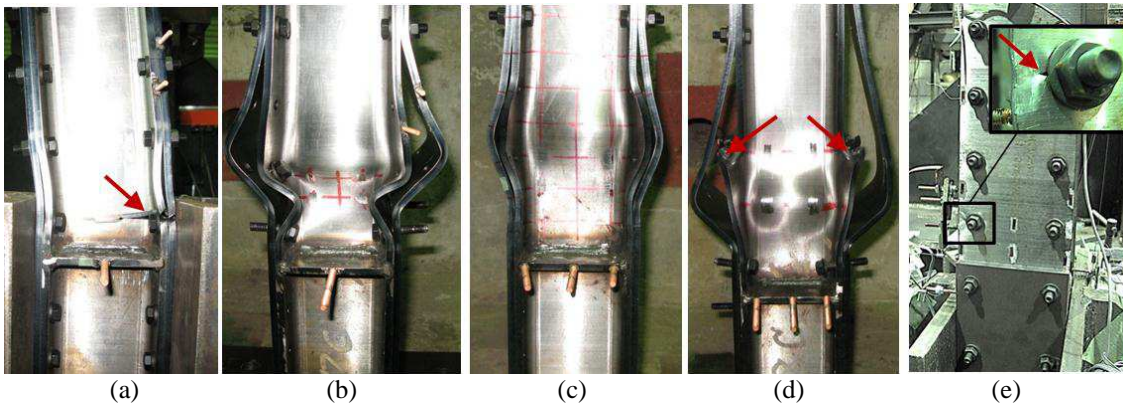


**Figure 4.** Final states of the specimens: (a) X60N0; (b) X60N2; (c) X60N4; (d) X120N2; (e) Y60N2.

Although all the specimens responded linearly under small rotation, the specimens exhibited different failure modes. The baseline specimen X60N2 yielded first, and then had local buckling at the rotation of about 0.06 rad (see Fig. 3(b)). Bolts at the buckled portion fractured as the loading continued, and the strength dropped sharply as the fractured bolts further aggravated the buckling. The local buckling mode is shown in Fig. 4(b). With no axial force, Specimen X60N0 only had slight local distortion at the rotation of 0.07 rad (see Fig. 4(a)) and fractured after two cycles of +0.75/-0.65 rad (see Fig. 3(a)). The tension-side exterior plate and the flanges of the channels fractured almost simultaneously at the first reduced section from the stiffeners), and spread to the webs immediately. Bearing larger axial force, Specimen X60N4 achieved smaller strength and deformation capacity, and local buckling and bolt rupture occurred in the cycle of +0.50/-0.50 rad (see Fig. 3(c)). With a double-length bolt pitch, Specimen X120N2 presented local buckling and bolt rupture earlier than the baseline specimen (see Fig. 3(d)), and fracture occurred in the compression-side flanges of internal channel due to the severe local buckling deformation (see Fig.4(d)). As a specimen loaded about the weak axis, Specimen Y60N2 exhibited stable strength growth after yielding. No local buckling was observed in Specimen Y60N2, and a small crack was observed at the edge of a bolt hole when loading was completed.

The column was demanded for large elastic deformation in the target structural system, so the elastic bending stiffness and yield rotation of the column are concerns for the design. Table 3 shows the values of the yield rotation, yield bending moment, and elastic stiffness from both of the test and estimation.  $M_{y,test}$  is the measured yield bending moment, defined as the moment at Section 1 when any of the measured strains at Sections 1 and 2 surpasses the yield strain. The yield rotation was obtained from Fig. 3 when the moment reached  $M_{y,test}$ .  $M_{y,r}$  is the estimated yield bending moment, calculated by  $M_{y,r} = F_y S_r$ , where  $S_r$  is the elastic section modulus of reduced section accounting for the bolt holes.

The measured elastic bending stiffness was obtained by fitting a straight line to the first  $\pm 0.01$  rad loading cycle of the curves in Fig. 3, while the estimated value was calculated by  $EI$ .  $E$  is the Young's modulus and  $I$  is the moment of inertia of the column gross section. Yield rotation indicates the limit of elastic deformation, and it grew as the axial force ratio decreased. The column was planned to be used under the axial force ratio of 0.2, and all the specimens with the axial force ratio of 0.2 achieved a yield rotation of over 0.018 rad, which is deemed large enough for the column to remain elastic in rare earthquake events. The measured stiffness of the column listed in Table 3 become smaller as the axial force ratio increases, which might be caused by the P-delta effect on the distribution of bending moment in the column. The values of the measured elastic stiffness are slightly smaller than the estimated value, and the maximum difference is within 7%, so the column can be taken as a solid-section column for the estimation of its elastic bending stiffness.

As shown in Table 3, the maximum difference between the measured and estimated yield strengths was 4% about the strong axis, and 6% about the weak axis.

**Table 3.** Test results and estimations

Specimen No.	$N/N_0$	Yield rot. (rad)	Bending moment (kN.m)			Elastic stiffness $EI$ (kN.m <sup>2</sup> )		
			$M_{y,test}$	$M_{y,r}$	$M_{y,test}/M_{y,r}$	Test	Est.	Test/Est.
X60N0	0.0	0.029	69.6	72.4	0.96	$1.201 \times 10^3$	$1.230 \times 10^3$	0.98
X60N2	0.2	0.021	55.5	55.3	1.00	$1.165 \times 10^3$	$1.230 \times 10^3$	0.95
X60N4	0.4	0.014	39.1	38.3	1.02	$1.149 \times 10^3$	$1.230 \times 10^3$	0.93
X120N2	0.2	0.021	54.8	55.3	0.99	$1.181 \times 10^3$	$1.230 \times 10^3$	0.96
Y60N2	0.2	0.018	27.0	25.4	1.06	$0.564 \times 10^3$	$0.590 \times 10^3$	0.96

Fig. 5 shows the measured yield bending moment and maximum moment (about the strong axis), and the estimated yield moments and plastic moments. The horizontal axis is the bending moment normalized by the estimated plastic moment of the reduced section under zero axial force, while the vertical axis is the axial force ratio. The solid and hollow markers (square or triangle) indicate the measured yield moment and maximum moment, respectively. The lines show the estimated values for both the net area of the reduced section and gross area of the full section. The estimated plastic moment was calculated assuming that all fibers of the reduced section reached measured yield stress  $F_y$ , either in tension or compression. The yield strength was inversely proportional to the magnitude of the axial force, and also as shown in Table 3, the estimated yield strength of the reduced section matched well with its corresponding measured values. The estimated yield strength can be used to identify the limit of elastic range.

The design goal was to achieve the plastic moment of the reduced section. The maximum moment of all tests exceeded the estimated plastic moment of the reduced section, although none reached the plastic moment of the gross section. The amount of the overstrength from the plastic moment of the reduced section varied in different specimens. As shown in Fig. 5, the specimen with a smaller bolt pitch achieved a larger maximum strength, e.g., the specimens under the axial force ratio of 0.2. When axial force ratio equalled to zero, the overstrength was caused mainly by the stress hardening of the material after yielding, and the maximum strength was limited by the fracture of the tension-side flange. As the axial force ratio increased, the overstrength became larger. The overstrength was not only caused by the stress hardening but also by the reason that the compressive resistance of the flange was not simply governed by the reduced section. The bolts participated in the compression of the flange after yielding, and the end plate at the bottom of the column further enhanced the

compression-side column flange at Section 1. For the loading about the weak axis, Specimen Y60N2 yielded at the moment of 27.0 kN.m and increased to its maximum moment of 53.3kN.m, which was almost twice the yield moment. The presence of larger strength increase about the weak axis was due to the shape effect of the section.

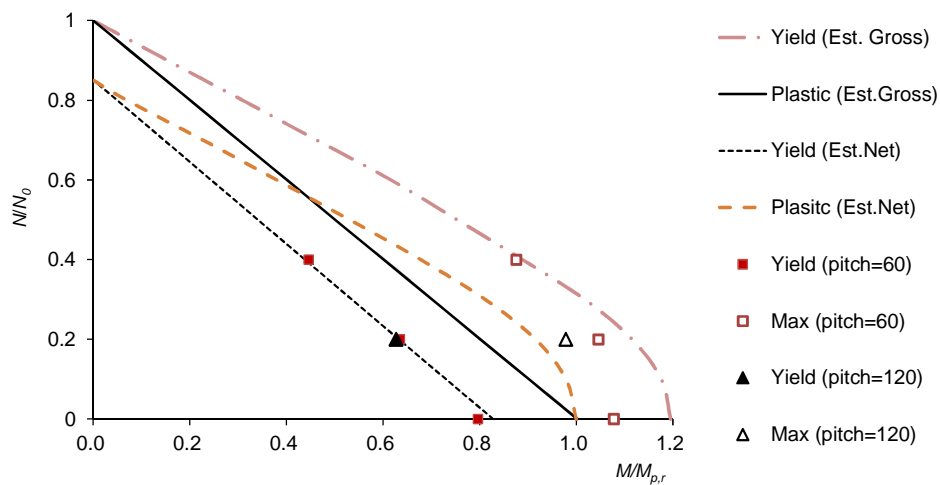


Figure 5. Yield strength and maximum strength (about the strong axis).

#### 4. CONCLUSIONS

The behavior of the column subjected to the combined bending and axial force was investigated with five specimens. The basic conclusions are as follows: (1) The column exhibited a very large yield rotation exceeding 0.018 rad under an axial force ratio of 0.2; (2) The elastic bending stiffness was within 7% to the estimated value based on the assumption that plane sections remain plane, and using the gross area of the section; (3) The strength of the column is limited by the net area of the reduced section; (4) The yield strength was inversely proportional to the axial force; (5) The flexural strength of the specimens exceeded the plastic moment of reduced sections using the measured yield strength of the steel.

The study is continuing to address the design method for the proposed built-up column and other design issues of related connection components, such as column base connections, column splices, and bracing connections.

#### ACKNOWLEDGEMENT

This paper reports a continuing research supported in part by the Japan Iron and Steel Federation.

#### REFERENCES

- Yoshida Y., Obinata T., Nishio M., Shiwaku T. (2009). Development of high-strength (780N/mm<sup>2</sup>) steel for building systems. *International Journal of Steel Structures* **9:4**, 285-289.
- Lin X., Chung Y.L., Okazaki T., Masayoshi, N. (2011). Weld-free columns using ultra-high-strength steel. Experimental study on flexural performance. *Proceedings of 6th European Conference on Steel and Composite Structures* **Vol C**.
- Lin X., Chung Y.L., Okazaki T., Masayoshi, N. (2012). Beam-to-column connection for built-up column using ultra-high-strength steel. *Proceedings of STESSA 2012*: 187-193.